

FES based wrist tremor suppression using multi-periodic repetitive control^{*}

Zan Zhang^{*} Bing Chu^{**} Yanhong Liu^{*} D.H. Owens^{*,***}

^{*} School of Electrical Engineering, Zhengzhou University, Zhengzhou, China (e-mail: zanzan@zzu.edu.cn, liuyh@zzu.edu.cn, d.h.owens@sheffield.ac.uk).

^{**} Department of Electronics and Computer Science, university of southampton, Southampton, SO17 1BJ, UK (e-mail: B.Chu@soton.ac.uk)

^{***} Department of Automatic Control and Systems Engineering, The University of Sheffield, Mappin Street, Sheffield, S1 3JD, UK

Abstract: Tremor is a very common motor disorder, mainly manifested as involuntary, periodic and rhythmic movement in any part of the body, especially in hands and upper-limbs, which seriously affects the life quality of patients. Functional electrical stimulation (FES) has been shown a promising technique to suppress tremor. Most existing FES based design methods assume tremor is a single frequency signal which however is a highly idealized simplification of the real case which contains multiple-frequency or even a frequency band, therefore limiting their practical performance. To address this problem, this paper proposes a controller design method based on multi-periodic repetitive control that is capable of suppressing tremor signal with multiple frequencies. Simulation and experimental results verify the effectiveness of the proposed method.

Keywords: Functional electrical stimulation (FES), tremor suppression, multi-periodic repetitive control, simulation and experimental verification.

1. INTRODUCTION

Tremor is an involuntary, rhythmic contraction of muscles, usually occurring in the hands and upper-limbs, which seriously affects the patient's voluntary movement and brings great difficulties to their daily life (Elble and Koller (1990)). It is a common complication of multiple sclerosis, stroke, Parkinson's disease. There are more than 40 million patients worldwide who are suffering from tremor caused by these three diseases (Collaborators (2019)). Therefore, it is urgent to find effective methods to suppress tremor.

A number of treatments have been proposed for tremor suppression, including invasive and non-invasive methods. Invasive method, such as deep brain stimulation, requires to implant electrodes in certain area of the brain. The cost of the surgery is high and the long-term efficacy also need to be further evaluated (Fishman et al. (2018)). The non-invasive methods include pharmacological treatment (Smits et al. (2017)), botulinum toxin injection (Brin et al. (2001)) and tremor suppression exoskeleton (Rocon et al. (2012)), etc. However, the above methods have some shortcomings, such as side effects of drugs, muscle rigidity after injection, and inconvenience and clumsiness in daily life, which limit their practical use. Functional electrical stimulation (FES) has been shown a promising method

for tremor suppression (Prochazka et al. (1992); Zhang et al. (2011); Copur et al. (2019)). In order to suppress tremor effectively by FES, one need to generate anti-phase moment with tremor movement by proper stimulating the associated muscles through surface electrodes.

So far, a variety of design methods have been proposed to regulate the electrical stimulation level. Conventional high-pass and bandpass filters were first adopted in FES based tremor suppression system. The experimental results showed that tremor attenuation rate can achieve 73% (Prochazka et al. (1992)). In Zhang et al. (2011), a neural oscillator was designed to suppress tremor by FES and PID feedback regulator was used to refine the intensity of stimulation. Simulation results showed that the tremor attenuation of 90% was achieved on average. Noticing that tremor signal is periodic, Copur et al (2019) used repetitive control (RC) to suppress tremor and the maximum tremor suppression at the specific tremor frequency can reach 93%.

While the above methods can improve the performance of tremor suppression, most of them are based on the assumption that tremor is approximately a periodic signal with single frequency. This however is a highly idealized simplification of the real scenario. Research results on various patients showed that tremor is a multiple frequency signals, or even a signal with frequency band (Zhou et al. (2018)). This paper proposes a multi-periodic repetitive control method to eliminate tremor signal with multiple frequencies. Firstly, a wrist musculoskeletal model with

^{*} This work is supported by the National Natural Science Foundation of China (No. 61803344, 61473265) and the Innovation Research Team of Science & Technology of Henan Province (No. 17IRTSTH-N013).

Hammerstein structure is developed, and the model parameters of different participants are identified individually. Then, the nonlinear wrist model is linearized and a frequency modified inverse multi-periodic repetitive control algorithm is proposed. The stability of the closed-loop system is proved as well. Finally the simulation and experiment are carried out to verify the performance of the proposed control method.

2. PROBLEM SET-UP

Tremor is a common disorder of motor function, which presents as involuntary, periodic and roughly sinusoidal movement. It can occur at any parts of human body, but mostly in the hands and forearms, such as the wrists. There are three degrees of freedom (DOF) of wrist motions, of which the wrist flexion and extension (WFE) movement occurs more commonly in daily life. This paper considers the tremor suppression related to WFE motion by FES method.

The principle of the FES based tremor suppression is applying weak electric current to the muscles to make them contraction and the associated joints producing opposite movement to tremor. In order to effectively suppress wrist tremor, we need to model and identify the musculoskeletal dynamics and adjust the level of FES applied to muscles by the controller design. The control system diagram of suppressing wrist tremor based on FES is shown in Fig. 1.

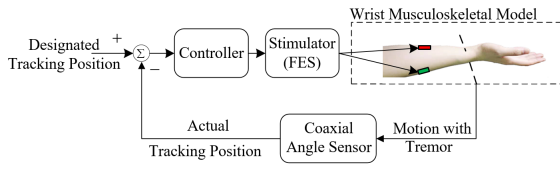


Fig. 1. The system diagram of suppressing wrist tremor based on FES

The FES based tremor suppression control system includes the controller, the stimulator, the angle sensor and the wrist dynamic model of patients. Tremor can be regarded as disturbance acting on the wrist dynamics. The angle sensor located in coaxial with wrist motion detects the real-time actual wrist joint tracking position. The aim of this paper is to design a feedback controller to minimize the error between the actual joint position and the designated tracking position. The FES level is adjusted by the controller to make the related muscles contraction through electrodes and to generate an anti-phase torque to suppress the tremor.

3. ELECTRICALLY STIMULATED WRIST MUSCULOSKELETAL MODEL

In order to design a feedback controller for tremor suppression, we need to model the wrist musculoskeletal dynamics first. Hammerstein structure is a widely used empirical muscle model in the field of bioengineering (Fengmin et al. (2010)). It consists of a nonlinear function representing muscle activation characteristics and a linear dynamic model. The static nonlinear function is often called as the isometric recruitment curve (IRC). The linear dynamic model presents the contraction properties of the muscles to

the electrical stimulation signal. The main muscles related to the wrist musculoskeletal model of WFE motion are Flexor carpi radialis (FCR) and extensor carpi radialis (ECR) muscle (Ramsay et al. (2009)). The electrically stimulated wrist musculoskeletal model is shown in Fig. 2.

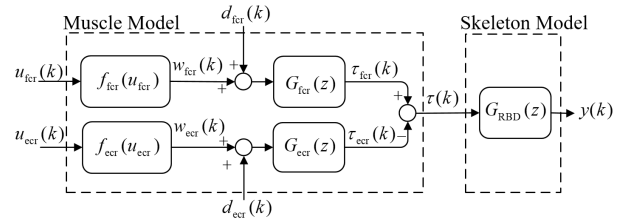


Fig. 2. Electrically stimulated wrist musculoskeletal model

The musculoskeletal model consists of three parts: muscle activation characteristics ($f_{fcr}(u_{fcr})$ and $f_{ecr}(u_{ecr})$), muscle contraction dynamics ($G_{fcr}(z)$ and $G_{ecr}(z)$) and skeletal dynamics ($G_{RBD}(z)$). The static muscle activation characteristics are often used to represent the stimulation inputs ($u_{fcr}(k)$ and $u_{ecr}(k)$) / steady-state isometric muscle torques output ($w_{fcr}(k)$ and $w_{ecr}(k)$) relationship. $d_{fcr}(k)$ and $d_{ecr}(k)$ are the tremor signals with multi-frequency. $\tau(k) = \tau_{fcr}(k) - \tau_{ecr}(k)$ is the overall moment; The output signal $y(k)$ of the system is the angle of WFE joint.

We first discuss muscle stimulation/activation characteristics. The typical isometric recruitment curves (IRCs) of the FCR and ECR muscles are shown in Fig. 3.

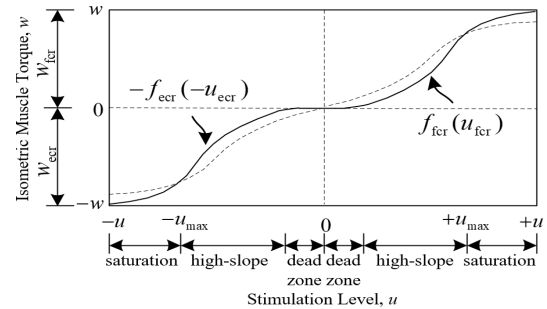


Fig. 3. IRCs of the FCR and ECR (solid line: no co-activation, dashed line: co-activation)

The IRCs of $f_{fcr}(\cdot)$ and $f_{ecr}(\cdot)$ are almost similar under the same stimulation level. In order to simplify the model structure and the related identification problem, two-input and two-output IRCs model is transformed into a single-input single-output model by combining the two inputs $u_{fcr}(k)$ and $u_{ecr}(k)$ into a single input $u(k)$. Then, the IRC model $f(u(k))$ can be formulated as

$$f(u(k)) = f_{fcr}(u_{fcr}(k)) - f_{ecr}(u_{ecr}(k))$$

$$= \begin{cases} f_{fcr}(u(k) + u_{c_{fcr}}) - f_{ecr}(u_{c_{ecr}}), & u(k) \in [0, 300 - u_{c_{fcr}}], \\ -(f_{ecr}(u_{c_{ecr}} - u(k)) + f_{fcr}(u_{c_{fcr}})), & u(k) \in [u_{c_{ecr}} - 300, 0], \end{cases} \quad (1)$$

where the maximum pulse width is set to $300\mu s$, since it provides a comfortable muscle contraction (Lyons et al. (2004)). $u_{c_{fcr}}$ and $u_{c_{ecr}}$ are the co-activation levels for FCR and ECR respectively. Co-activation refers to the co-activation of agonists and antagonists to ensure the posture stability of wrist movement, however the level

of co-activation should be selected the minimal values to avoid impeding voluntary movement. If $u_{c_{fcr}} = u_{c_{ecr}} = 0$, the dead zone of IRCs can't be removed, as shown in Fig. 3 (the solid line). If there is co-activation effect, i.e., $u_{c_{fcr}}, u_{c_{ecr}} \neq 0$, the dead zone of IRCs is removed, as shown in Fig. 3 (the dashed line). Let $f_{fcr}(u_{c_{fcr}}) = f_{ecr}(u_{c_{ecr}})$ with $f(0) = 0$, $f(u(k))$ is continuous and monotonic increasing recruitment curve and has definable inverse. The IRC model takes the form of

$$f(u(k)) = r_0 + r_1 u + r_2 u^2 + \dots + r_s u^s. \quad (2)$$

If it satisfies

$$\frac{df(u(k))}{du} = r_1 + 2r_2 u + \dots + s r_s u^{s-1} \geq 0, \quad (3)$$

the recruitment curve is monotonic, where s is the order of static nonlinear function and r_0, r_1, \dots, r_s are the nonlinear parameters need to be identified.

$d_{fcr}(k)$ and $d_{ecr}(k)$ are multiple periodic signals with period N_p ($p = 1, 2, \dots, n$) and can be assumed to contain a maximum N_f harmonic. And hence their sum $d(k)$ is also given by the N_p -periodic signal.

Due to the similar biophysical properties of the wrist flexors and extensors (Colacino et al. (2012)), we assume that the FCR and ECR have approximate linear contraction dynamics, that is, $G_{fcr}(z) \approx G_{ecr}(z)$, denoted as $G_L(z)$. Further noticing that the skeletal dynamics of limbs, in which the damping and elastic functions are linear, so we can combine $G_L(z)$ and $G_{RBD}(z)$ to get an equivalent linear musculoskeletal model $P(z)$. The transfer function $P(z)$ takes the form of

$$P(z) = \frac{B(z^{-1})}{A(z^{-1})} = \frac{b_1 z^{-1} + \dots + b_{n_b} z^{-n_b}}{1 + a_1 z^{-1} + \dots + a_{n_a} z^{-n_a}}, \quad (4)$$

where b_1, \dots, b_{n_b} , and a_1, \dots, a_{n_a} are parameters to be identified.

4. REPETITIVE CONTROL FOR WRIST TREMOR SUPPRESSION

The closed feedback control diagram is shown in Fig. 4, where $r(k)$ is the designated tracking position, $y(k)$ is the output angle of wrist motion, $e(k)$ is the error between $r(k)$ and $y(k)$. Due to the wrist musculoskeletal model is nonlinear, a feed-forward controller is first designed to linearize the system. The recruitment nonlinearity $f(u)$ is invertible, therefore, it can be cancelled by the inverse function of $f^{-1}(\bar{w})$. Then, we construct a multi-periodic feedback repetitive controller to improve the performance of the tremor suppression.

4.1 Design of repetitive controller

Tremor signals can be seen as multi-periodic disturbance. RC method embeds internal models (IM) to enable exact cancellation of the repeating disturbance (N_p -periodic signal $d(k)$), so the output of the closed loop system can reject disturbances acting on the system completely. The multi-periodic repetitive controller is presented as follows

$$C(z) = \left(1 + \sum_{p=1}^n \frac{z^{-N_p}}{1 - z^{-N_p}} K_p\right) H(z), \quad (5)$$

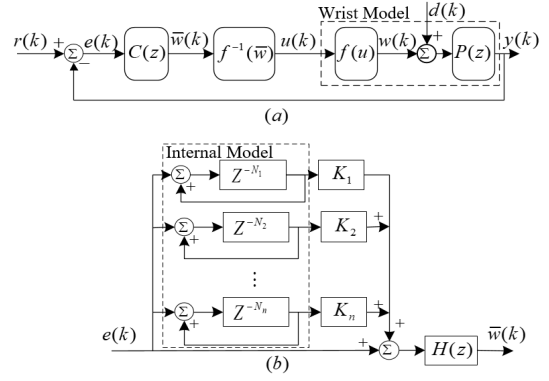


Fig. 4. (a) The closed feedback RC system, (b) The multi-periodic repetitive controller $C(z)$

where K_p is the gain of each repetitive control loop, $\sum_{p=1}^n \frac{z^{-N_p}}{1 - z^{-N_p}}$ is the multi-periodic internal models. $N_p = T_p/T_s$, where T_p is the period of loop p and T_s is the sampling period of the controller. $H(z)$ is a compensator that can improve the stability and dynamic performance of the system.

Theorem 1: Under the multi-periodic repetitive controller (5), the system depicted in Fig. 4 is asymptotically stable and the multi-periodic disturbances can be rejected if the control gains $K_p > 0$ and the compensators $H(z)$ is chosen such that the following equation has all roots in the unit circle

$$1 + P(z)H(z)\left(1 + \sum_{p=1}^n \frac{z^{-N_p}}{1 - z^{-N_p}} K_p\right) = 0. \quad (6)$$

Especially, when $H(z) = P(z)^{-1}$, the above condition becomes

$$\sum_{p=1}^n K_p < 4. \quad (7)$$

Proof: From the internal model principle, we can see that the proposed controller (5) can reject multi-frequency disturbance. The characteristic equation of the closed loop system can be written as (6). If $K_p > 0$ and Equ. (6) has all roots in the unit circle, the closed loop system is asymptotically stable.

When $H(z) = P(z)^{-1}$, (6) can be reformulated as

$$2 + \sum_{p=1}^n \frac{z^{-N_p}}{1 - z^{-N_p}} K_p = 0. \quad (8)$$

Following the similar procedure presented in Chang et al. (1998), the system is asymptotically stable if

$$Re\left(\frac{z^{-N_p}}{1 - z^{-N_p}}\right) < -\frac{1}{2}. \quad (9)$$

From (8), we have

$$0 = Re\left(2 + \sum_{p=1}^n \frac{z^{-N_p}}{1 - z^{-N_p}} K_p\right) < 2 - \frac{1}{2} \sum_{p=1}^n K_p, \quad (10)$$

that is,

$$\sum_{p=1}^n K_p < 4.$$

Thus complete the proof. ■

4.2 Frequency modified inverse RC

Due to the parameter uncertainties, the inverse of $P(z)$ is often unrealizable. In this subsection, frequency modified inverse multi-periodic repetitive control (FMI-MP-RC) is used to obtain the order and parameters of $H(z)$. According to Longman (2010), $H(e^{i\omega_j T})$ can approximate the inverse of the frequency response of the system by minimizing the following cost function

$$J = \sum_{j=0}^{N_p} [1 - P(e^{i\omega_j T})H(e^{i\omega_j T})][1 - P(e^{i\omega_j T})H(e^{i\omega_j T})]^*, \quad (11)$$

where

$$H(z) = c_1 z^{m-1} + c_2 z^{m-2} + \dots + c_m z^0 + \dots + c_{n-1} z^{-(n-m-1)} + c_n z^{-(n-m)}, \quad (12)$$

m and n are positive integers and ω_j is a discrete set of frequencies selected from zero to Nyquist frequency. Let $M_P(\omega_j)$ and $\varphi_P(\omega_j)$ be the magnitude and phase of $P(e^{i\omega_j T})$ respectively. Substituting (12) into (11), we get a set of linear equations $D\mathbf{c} = \mathbf{b}$, where

$$D = \sum_{j=0}^N M_P^2(\omega_j) \times \Theta, \quad (13)$$

$$\mathbf{b} = \sum_{j=0}^N M_P(\omega_j) \times \begin{bmatrix} \cos((m-1)\omega_j T + \varphi_P(\omega_j)) \\ \cos((m-2)\omega_j T + \varphi_P(\omega_j)) \\ \dots \\ \cos((m-n)\omega_j T + \varphi_P(\omega_j)) \end{bmatrix}, \quad (14)$$

$$\Theta = \begin{bmatrix} 1 & \cos(\omega_j T) & \dots & \cos((n-1)\omega_j T) \\ \cos(\omega_j T) & 1 & \dots & \cos((n-2)\omega_j T) \\ \vdots & \vdots & \ddots & \vdots \\ \cos((n-1)\omega_j T) & \cos((n-1)\omega_j T) \dots & & 1 \end{bmatrix}. \quad (15)$$

The parameters $\mathbf{c} = [c_1 \ c_2 \ \dots \ c_n]^T$ in the compensator $H(z)$ can be got by solving the equations $D\mathbf{c} = \mathbf{b}$.

5. EXPERIMENTAL VERIFICATION

5.1 Experimental platform

In order to verify the FMI-MP-RC algorithm for multi-frequency wrist tremor suppression and identify the parameters of the wrist musculoskeletal Hammerstein model individually (Ethical approval was obtained from the Zhengzhou University, China. (No.ZZURIB2019-004)), an FES-based tremor suppression experimental platform is set up, as shown in Fig. 5.

The experimental platform embeds an artificial tremor generator, so the experiments can be carried on the participants without wrist tremor disease. The hand and forearm of participant are supported by U-shaped splint (U2-Splint and U1-Splint), the wrist and forearm are fixed to prevent any movement of the elbow joint and only to generate wrist flexion and extension plane motion. Different frequencies of tremor signals can be generated by DC motor and the torque of DC motor is transmitted to the participant by shaft. The encoder is mounted on the shaft and the encoder

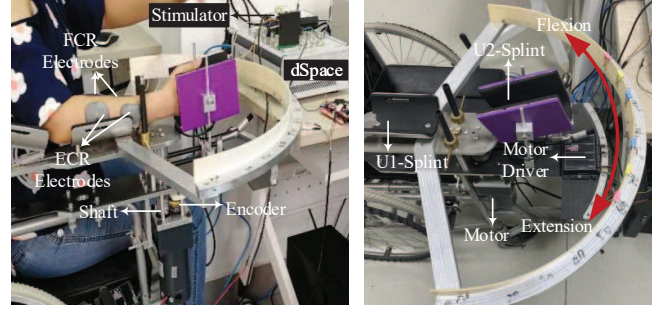


Fig. 5. Experimental platform for wrist tremor suppression

can obtain the WFE motion angle of the participant according to the rotation of the shaft. The encoder data is transmitted to hardware dSpace 1202 in real-time, which can interface directly with Matlab/Simulink. The FMI-MP-RC algorithm proposed above is utilized to generate the corresponding FES signals to the electrical stimulator to suppress multi-frequency tremor.

5.2 Identification of the wrist model

As shown in Fig. 5 (a), two surface electrodes are placed on FCR and ECR muscles respectively before starting an experiment. The experiment of parameters identification consists of two steps.

Nonlinear Parameters Estimation: Peak impulse response method is used to estimate nonlinear parameters of IRC. Input signals are the single stimulus pulse with different pulse widths ($50\mu s$, $100\mu s$, $150\mu s$, $200\mu s$, $250\mu s$ and $300\mu s$) and the outputs are the peak values of muscle impulse response. The whole identification process takes less than two minutes. The quadratic programming approach can be used to solve this optimal problem and get the parameters and order of IRC.

Linear Parameters Identification: In order to generate test data for estimating the linear part of the muscle model, the approximated recruitment nonlinearity is eliminated via the inverse function, as shown in Fig. 4 (a). All the parameters of formula (4) and tremor signals are rewritten in a explicit form and denote it as θ . The $d(k)$ can be written in the following matrix form,

$$d(k) = [1 \ \cos(\frac{2\pi k}{N_1}) \dots \sin(\frac{2\pi N_f k}{N_p})][\lambda_0 \ \lambda_{11}^A \dots \lambda_{pN_f}^B]^T = h_v \theta_v. \quad (16)$$

Let

$$\theta = [a_1, a_2, \dots, a_{n_a}, b_1, b_2, \dots, b_{n_b}, \theta_v]^T, \\ h(k) = [-y(k-1), \dots, -y(k-n_a), \dots, u(k-n_b), h_v],$$

the linear dynamics can be written as $y(k) = h(k)\theta$. The consistency and unbiased estimation of θ can be obtained by the LS identification algorithm.

5.3 Simulation testing and analysis

In this subsection we carry out simulation to test and verify the effectiveness of the proposed FMI-MP-RC algorithm for wrist multi-frequency tremor suppression. The results of FMI-MP-RC, frequency modified inverse single

periodic RC (FMI-SP-RC) and the conventional PID high-pass filter (PID-HF) feedback control will be compared.

The tremor data is collected from different tremor patients in department of rehabilitation, the Fifth Affiliated Hospital of Zhengzhou University. The WFE motion datas of tremor patients were collected by the experimental platform. The frequency spectrum of the tremor signal is shown in Fig. 6. It can be seen that the tremor signal is multi-frequency and has two main peaks with different amplitudes.

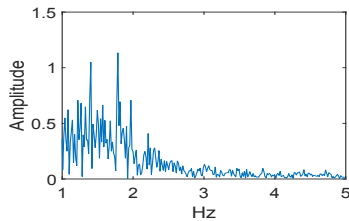


Fig. 6. The typical spectrum of WFE motion

During simulation testing, the multi-periodic disturbance $d(k)$ are set to sinusoidal wave with two frequencies. The frequencies are 2Hz, 2.5Hz and the amplitudes are 1, 0.4 respectively. Sample period T_s is 0.005s. The gains of the RC controller are chosen as $K_1 = K_2 = 0.5$. The orders and parameters of the participant musculoskeletal model $f(u)$ and $P(z)$ are obtained by experimental platform. The internal model of FMI-SP-RC includes 2Hz single frequency tremor signal, which is the major components. The optimized parameters of PID-HF regulator is determined by trial and error method. The parameters of filter order and cut-off frequency of high-pass Butterworth filter are selected as 6th and 1.2Hz respectively. We set $r(k) = 0$ and the output $y(k)$ tracks the tremor signals $d(k)$. The steady state time is chosen as 15s to 20s. The parameters of m and n of compensator $H(z)$ are selected by minimizing cost function (11). Then we use the following tracking error performance (root mean square error, RMSE)

$$\text{RMSE} = \|d - y\|_2, \quad (17)$$

and steady-state error performance (maximum steady-state error, MSSE)

$$\text{MSSE} = \frac{\|y - r\|_\infty}{\|d\|_\infty}, \quad (18)$$

to quantify the performance of each control algorithm on tremor suppression, where d is the tremor signal, y is the output signal, r is the reference signal. RMSE and MSSE values of the simulation results are shown in Table. 1.

It can be seen from Table. 1 that the RMSE values of FMI-MP-RC are much smaller than those of FMI-SP-RC and PID-HF. It means that the output of the system can track the multi-periodic tremor signal by FMI-MP-RC algorithm. In the last 5 seconds of simulation, the MSSE values of FMI-MP-RC tend to zero, while the MSSE values of the other two control algorithms can not converge to zero. Moreover, the MSSE values of the RC methods are less affected by the change of the controller parameters, while the MSSE value of the PID-HF algorithm is greatly affected by the change of the controller parameters. In summary, FMI-MP-RC method can suppress multi-periodic tremor signal significantly.

Table 1. Simulation results with different controller parameters

Controller Type	Controller Parameters	RMSE	MSSE
FMI-MP-RC	m=41,n=35	0.1454	0.0015
	m=53,n=47	0.1347	4.1348×10^{-4}
	m=61,n=55	0.1149	2.5598×10^{-4}
FMI-SP-RC	m=41,n=35	0.3146	0.2027
	m=53,n=47	0.3213	0.2007
	m=61,n=55	0.3311	0.2056
PID-HF	P=70,I=70	0.4643	1.2119
	P=65,I=65	0.4542	0.8957
	P=60,I=60	0.4643	0.7960

FMI-SP-RC method can suppress single frequency (2Hz) tremor signal, but can not attenuate the tremor signal of 2.5Hz. The traditional PID-HF controller can not suppress the tremor signal effectively.

5.4 Experimental validation

In this subsection, the tremor suppression performance of the three proposed control algorithms are verified by the self-designed experimental platform. The following three tests are considered during the experiment.

Test 1 (T1): Tracking task without induced tremor and FES.

Test 2 (T2): Tracking task with induced tremor but without FES.

Test 3 (T3): Tracking task with induced tremor and FES. The experimental results of the three control algorithms proposed above are shown in Fig. 7.

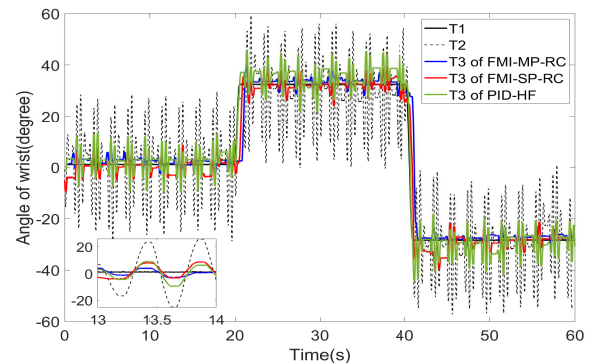


Fig. 7. WFE motion tracking (T1, T2 and T3) with FMI-MP-RC, FMI-SP-RC and PID-HF methods

It can be seen from Fig. 7 that the tremor suppression performance of FMI-MP-RC algorithm is better than the other two methods. RMSE, MSSE and the tremor suppression rate (TSR) are used to describe the tremor suppression performance more clearly. TSR is defined as follows,

$$\text{TSR} = \frac{\|d - y\|_2}{\|r - y\|_2}, \quad (19)$$

where d is the output signal of T2, y is the output signal of T3, r is the output signal of T1. The performance of tremor suppression under different control methods are shown in Table. 2.

As shown in Table 2, The RMSE and MSSE values under FMI-SP-RC and PID-HP are much greater than FMI-MP-RC method, which is consistent with the simulation

Table 2. Experimental results with different controllers

Controller Type	RMSE	MSSE	TSR
FMI-MP-RC	3.1182	1.2967	95.72%
FMI-SP-RC	6.8355	7.3281	79.42%
PID-HF	7.9910	10.4375	71.85%

results. The steady state error under FMI-MP-RC is less than the tracking error, which shows that this method can eliminate the multi-frequency tremor signals effectively. The MSSE values under FMI-SP-RC and PID-HF algorithms are both greater than RMSE values. It represents that when the system reaches the steady state, neither of them has good performance of suppressing multi-periodic tremor. The TSR value under FMI-MP-RC algorithm is up to 95.72%, while the other two control algorithms can only achieve 79.42% and 71.85% respectively. In summary, the repetitive control algorithm based on multiple internal models proposed in this paper can suppress the multi-periodic tremor signal more effectively.

6. CONCLUSION

This paper proposed a multi-periodic repetitive controller based on FES to suppress wrist tremor with multiple frequencies. The nonlinear Hammerstein structure is used to model the wrist musculoskeletal system. The parameters of each participant are identified individually. Then a feed-forward controller is utilised to linearize the wrist model first and multi-periodic repetitive control is proposed to suppress multi-frequency tremor signal. Simulation and experimental results show that the proposed FMI-MP-RC method can effectively improve the performance of multiple frequencies tremor suppression.

While the above results are promising, there are some issues need to be investigated. 1. Robust RC design: Due to modelling errors or the unmodelled high frequency dynamics, the robust performance of the repetitive controller will be considered in the future work. 2. Adaptive RC design: The tremor frequency may change over time, the design of adaptive repetitive controller based on frequency variation can obtain better performance of tremor suppression and improve the practical application value of the system. 3. Lower order multi-periodic RC design: The problem of optimal RC will be explored in multi-frequency tremor suppression system. A lower order multi-periodic RC will be developed to improve computational efficiency. 4. Clinical trails: Current experiments were conducted on participants without tremor disease. After successful evaluation with unimpaired participants, clinical trails can be undertaken with tremor patients.

REFERENCES

- Brin, M.F., Lyons, K.E., Doucette, J., Adler, C.H., Caviness, J.N., Comella, C.L., Dubinsky, R.M., Friedman, J.H., Manyam, B.V., and Matsumoto, J.Y. (2001). A randomized, double masked, controlled trial of botulinum toxin type a in essential hand tremor. *Neurology*, 56(11), 1523–1528.
- Chang, W.S., Suh, I.H., and Oh, J.H. (1998). Synthesis and analysis of digital multiple repetitive control systems. In *American Control Conference*, volume 5, 2687–2691.
- Colacino, F.M., Emiliano, R., and Mace, B.R. (2012). Subject-specific musculoskeletal parameters of wrist flexors and extensors estimated by an emg-driven musculoskeletal model. *Medical Engineering & Physics*, 34(5), 531–540.
- Collaborators, G..N. (2019). Global, regional, and national burden of neurological disorders, 1990-2016: a systematic analysis for the global burden of disease study 2016. *The Lancet. Neurology*, 18, 459–480.
- Copur, E.H., Freeman, C.T., Chu, B., and Laila, D.S. (2019). Repetitive control of electrical stimulation for tremor suppression. *IEEE Transactions on Control Systems Technology*, 27(2), 540–552.
- Elble, R. and Koller, W. (1990). *Tremor*. The Johns Hopkins University Press.
- Fengmin, L., Markovskiy, I., Freeman, C.T., and Rogers, E. (2010). Identification of electrically stimulated muscle models of stroke patients. *Control Engineering Practice*, 18(4), 396–407.
- Fishman, P.S., Elias, W.J., Ghanouni, P., Gwinn, R., Lipsman, N., Schwartz, M., Chang, J.W., Taira, T., Krishna, V., and Rezai, A. (2018). Neurological adverse event profile of magnetic resonance imaging-guided focused ultrasound thalamotomy for essential tremor. *Movement Disorders*, 33(5), 843–847.
- Longman, R.W. (2010). On the theory and design of linear repetitive control systems. *European Journal of Control*, 16(5), 447–496.
- Lyons, G., Leane, G., Clarke-Moloney, M., O'Brien, J., and Grace, P. (2004). An investigation of the effect of electrode size and electrode location on comfort during stimulation of the gastrocnemius muscle. *Medical Engineering & Physics*, 26(10), 873–878.
- Prochazka, A., Elek, J., and Javidan, M. (1992). Attenuation of pathological tremors by functional electrical stimulation I: Method. *Annals of Biomedical Engineering*, 20(2), 205–224.
- Ramsay, J.W., Hunter, B.V., and Gonzalez, R.V. (2009). Muscle moment arm and normalized moment contributions as reference data for musculoskeletal elbow and wrist joint models. *Journal of Biomechanics*, 42(4), 463–473.
- Rocon, E., Gallego, J.I., Belda-Lois, J.M., Benito-Len, J., and Pons, J.L. (2012). Biomechanical loading as an alternative treatment for tremor: A review of two approaches. *Tremor & Other Hyperkinetic Movements*, 2, 601–603.
- Smits, E.J., Tolonen, A.J., Cluitmans, L., Gils, M.V., Zietsma, R.C., Borgemeester, R.W.K., Laar, T.V., and Maurits, N.M. (2017). Graphical tasks to measure upper limb function in patients with parkinsons disease: Validity and response to dopaminergic medication. *IEEE Journal of Biomedical & Health Informatics*, 21(1), 283–289.
- Zhang, D., Poignet, P., Widjaja, F., and Wei, T.A. (2011). Neural oscillator based control for pathological tremor suppression via functional electrical stimulation. *Control Engineering Practice*, 19(1), 74–88.
- Zhou, Y., Jenkins, M.E., Naish, M.D., and Trejos, A.L. (2018). Characterization of parkinsonian hand tremor and validation of a high-order tremor estimator. *IEEE Transactions on Neural Systems and Rehabilitation Engineering*, 26(9), 1823–1834.